Hydrol. Earth Syst. Sci. Discuss., 9, 10303–10322, 2012
www.hydrol-earth-syst-sci-discuss.net/9/10303/2012/
doi:10.5194/hessd-9-10303-2012

Hydrology and Earth System Sciences Discussions

A universal calibration function for determination of soil moisture with cosmic-ray neutrons

T. E. Franz, M. Zreda, R. Rosolem, and T. P. A. Ferre

Department of Hydrology and Water Resources, University of Arizona, 1133 East James E. Rogers Way, Room 122, Tucson, Arizona 85721, USA

Received: 29 August 2012 – Accepted: 30 August 2012 – Published: 11 September 2012

Correspondence to: T. E. Franz (tfranz@email.arizona.edu)

Published by Copernicus Publications on behalf of the European Geosciences Union.

Abstract

A cosmic-ray soil moisture probe is usually calibrated locally using soil samples collected within its support volume. But such calibration may be difficult or impractical, for example when soil contains stones, in presence of bedrock outcrops, in urban environments, or when the probe is used as a rover. Here we use the neutron transport code MCNPx with observed soil chemistries and pore water distribution to derive a universal calibration function to be used in such environments. Comparisons with independent soil moisture measurements at one cosmic-ray probe site and, separately, at thirty-five sites, show that the universal calibration function explains more than 75 % of the total variation within each dataset, permitting accurate isolation of the soil moisture signal from the measured neutron signal.

1 Introduction

Understanding the exchange of water between the land surface and atmosphere is critical for accurate initialization of general circulation models (Koster et al., 2004; Wang et al., 2006), understanding energy and water fluxes (Seneviratne et al., 2010), and thus making short-term weather predictions. However, accurate and exhaustive soil moisture datasets in space and time are difficult to obtain (Robinson et al., 2008), hindering progress in fundamental understanding of the land-atmosphere coupling (Jung et al., 2010; Seneviratne et al., 2010). The recently-developed cosmic-ray soil moisture method (Zreda et al., 2008) and probe by Hydroinnova LLC, Albuquerque, NM, USA, allow for near surface soil moisture measurements (~ 12 to 70 cm) at intermediate horizontal scales (~ 36 ha) (Desilets et al., 2010). Fifty probes have been deployed around the continental USA as part of the COsmic-ray Soil Moisture Observing System (COSMOS) (Zreda et al., 2012; data available at http://cosmos.hwr.arizona.edu/), and other networks are being installed elsewhere.

HESSD

9, 10303–10322, 2012

Previous work has concentrated on the relation between the neutron intensity in air above the land surface and soil moisture. However, that intensity is influenced not only by soil moisture, but also by hydrogen in other reservoirs. Desilets et al. (2010) presented a theoretical calibration function that required at least one independent estimate of area-average soil moisture to define the free parameter, N_0. Analysis of thirty-five different COSMOS site calibration datasets indicates that N_0 varies significantly from site to site and in time within the same site (Table S1) due to presence of other time varying sources of hydrogen, such as fast-growing corn (Hornbuckle et al., 2012).

While it is possible to collect soil calibration datasets at some sites, at others it may be impossible (e.g. where soils contain stones, where rocks outcrops are present, in urban environments, in inaccessible areas, etc.), or impractical (e.g. for large-scale mobile surveys, Desilets et al., 2010). However, water is still exchanged between the land surface and atmosphere at these sites, and observations of area-average moisture are necessary to understand the transfer of mass, momentum, and energy in these systems. Such observations may be possible with the aid of a universal calibration function.

Universal calibration functions and algorithms have been developed in the past, with some of them being transformative in terrestrial hydrology. For example, Knyazikhin et al. (1998), utilized a radiative transfer model in six different vegetation classes to derive a global leaf area index and fraction of absorbed photosynthetically active radiation from satellite derived spectroradiometer measurements. Topp et al. (1980), found a single relationship between the measured dielectric constant and volumetric water content across a wide range of soil types using coaxial transmission lines.

In this work, we develop a universal calibration function for the cosmic-ray neutron probe. It accounts for several sources of time varying hydrogen signals that may be present in the probe's support volume in order to expand the potential use of the probe to hitherto difficult sites and novel applications. We first develop the function using the neutron transport code MCNPx (Pelowitz, 2005), for two different cases: uniform variations of pore water in fifty different soil chemistries, and vertical variations in pore water

HESSD
9, 10303–10322, 2012

in four different soil textures using a numerical solution to the 1-D Richards equation. We then test the validity of the function by using observed neutron data from thirty-five COSMOS sites (where we have full calibration datasets) with a wide range of conditions.

2 Methods

2.1 Relationship between low-energy neutron intensity and hydrogen

The intensity of low-energy neutrons in air above the land surface is controlled mainly by the number of atoms of hydrogen in the combined soil-air system (Zreda et al., 2008). Hydrogen at the surface is present in three forms: static (soil mineral structure, mostly constant in time), quasi-static (vegetation, possibly varying in time) and transient (water vapor, pore or ponded water, snow, all changing in time). The support volume of a cosmic-ray probe is governed by the average travel distance of neutrons in air near the land surface (Desilets et al., 2010). Because of the additional sources of hydrogen, it is difficult to isolate a single transient signal (here, soil moisture) from the convoluted detected signal (here, neutron intensity) without additional information, constraints or simplifications.

The influence of additional sources of hydrogen is evident from the wide range of N_0 values computed for COSMOS sites using the Desilets et al. (2010) calibration function:

$$\theta(N) = \frac{0.0808}{\left(\frac{N}{N_0}\right) - 0.372} - 0.115 \quad (1)$$

where θ is the volumetric pore water content ($m^3\,m^{-3}$), N is the neutron counting rate/flux normalized to a reference atmospheric pressure and solar activity level and N_0 is the counting rate/flux over dry soil under the same reference conditions. Using

HESSD
9, 10303–10322, 2012

Calibration function for soil moisture determination with cosmic-ray neutrons

T. E. Franz et al.

forty-five calibration datasets from thirty-five different COSMOS sites we find N_0 varies significantly (mean = 2632 counts per hour, cph, st. dev. = 433 cph, min. = 1892 cph, max. = 3394 cph; Table S1). This parameter should be approximately constant when accounting for all hydrogen sources; therefore the large spread indicates that not all sources of hydrogen are taken into account.

2.2 A practical framework

Given the deficiency of Eq. (1) to account for additional or time varying hydrogen signals, we present a simplified but general framework to account for all hydrogen sources present. We assume that a monotonic relationship exists between observed neutrons and the amount of hydrogen present in the support volume. In order to isolate the different transient signals, we employ neutron intensity correction factors and assign average properties within the support volume. From neutron transport simulations, Zreda et al. (2008) found that 86 % of the neutron signal occurs within a 335 m radius and is nearly independent of soil moisture. They also found that the vertical extent of the neutron signal depends on soil moisture, ranging from 12 cm in wet soils ($0.40\,m^3\,m^{-3}$) to 70 cm in dry ones ($0\,m^3\,m^{-3}$).

In the air, the support volume is approximately a hemisphere with a radius of 335 m. The neutron signal is normalized to the same reference pressure, geomagnetic latitude, and the incident high-energy neutron intensity as summarized in Zreda et al. (2012) and implemented in the COSMOS project (Level 2 data available at http://cosmos.hwr.arizona.edu/). In addition, the neutron signal is corrected for variations in atmospheric water vapor (Rosolem et al., 2012; Zreda et al., 2012):

$$\mathrm{CWV} = 1 + 0.0054\left(\rho_v^0 - \rho_v^{\mathrm{ref}}\right) \tag{2}$$

where CWV is the scaling factor for temporal changes in cosmic-ray intensity as a function of changes in atmospheric water vapor ($N \times \mathrm{CWV}$), ρ_v^0 ($g\,m^{-3}$) is the absolute water vapor at the surface, and ρ_v^{ref} ($g\,m^{-3}$) is the absolute water vapor at the surface at a

HESSD
9, 10303–10322, 2012

reference condition (here we use dry air, $\rho_v^{ref} = 0$). Estimates of absolute humidity can be made with surface measurements of air temperature, air pressure, and relative humidity following Rosolem et al. (2012) (see Table S1).

In the subsurface, the support volume is a cylinder with a fixed radius of 335 m and a depth that varies with soil moisture content. In order to calculate the measurement depth and depth-weighted average of properties within the volume, we adopt the framework outlined in Franz et al. (2012a). For uniform distributions of pore water, lattice water, and bulk density, Franz et al. (2012a) found the effective depth z^* (cm) as:

$$z^* = \frac{5.8}{\frac{\rho_{bd}}{\rho_w}\tau + \theta + 0.0829} \quad (3)$$

where 5.8 (cm) represents the 86 % cumulative sensitivity depth of low-energy neutrons in liquid water, 0.0829 is controlled by the nuclear cross sections of SiO_2, ρ_{bd} is the dry bulk density of soil ($g\,cm^{-3}$), ρ_w is the density of liquid water assumed to be 1 ($g\,cm^{-3}$), and τ is the weight fraction of lattice water in the mineral grains and bound water, defined as the amount of water released at 1000 °C preceded by drying at 105 °C (g of water per g of dry minerals, also known as lattice water, Actlabs, Ontario, Canada).

With the estimates of sensor support volume and average properties within that volume, the total mass in the system and the total number of moles of each element can be calculated (Table S1). Following the neutron correction factor for variations in atmospheric water vapor (Eq. 2), we assume the atmosphere is composed of only nitrogen (79 % by weight) and oxygen (21 % by weight). We estimate wet above ground biomass, AGB ($kg\,m^{-2}$), from US Forest Service maps (http://webmap.ornl.gov/biomass/biomass.html) and assume vegetation is only composed of water (60 % by weight) and cellulose ($C_6H_{10}O_5$, 40 % by weight). We assume the subsurface is composed of solid grains (pure quartz, SiO_2, plus lattice water) and pore water. With the estimates of volume, mass, and chemical composition, hydrogen molar fraction, hmf ($mol\,mol^{-1}$), is:

HESSD
9, 10303–10322, 2012

$$\text{hmf} = \frac{\sum H_i}{\sum A_i} \quad (4)$$

where H_i is the sum of hydrogen moles from pore water, lattice water, and vegetation inside the support volume, and A_i is the sum of all moles from pore water, lattice water, vegetation, soil, and air inside the support volume. Table S1 presents a summary of all calculations from the forty-five calibration datasets at thirty-five different COSMOS locations (some locations have more than one calibration data set).

2.3 Modeled neutron intensity for variations in soil mineral chemistry

To simulate the transport of cosmic-ray particles through the atmosphere and shallow subsurface we used the MCNPx model (Pelowitz, 2005), a general purpose Monte Carlo code that tracks the individual life history of a particle and subsequent particles as it interacts with matter. At 1 to 2 m above the surface the fast neutron flux, N (energy range 10–100 eV), is tallied; it corresponds to the same energy neutrons that are measured by a cosmic-ray neutron detector. The neutron transport simulations used soil mineral chemistries from fifty COSMOS sites (Table S2) combined with twelve different uniformly distributed pore water values (Fig. 1). Despite large variations in soil chemistry (most notably lattice water), the framework presented in Sect. 2.2 explained 99 % of the variation (Table 1) between relative neutron flux and hydrogen molar fraction within the sensor support volume using a two term exponential function:

$$\frac{N}{N_s} = 4.486 \exp(-48.1 \times \text{hmf}) + 4.195 \exp(-6.181 \times \text{hmf}) \quad (5)$$

In all simulations, neutron flux is normalized to the case of an infinitely deep layer of water beneath the sensor (i.e. no soil). The modeled neutron intensity over pure quartz is 8.5 times higher than that over water, which is similar to the theoretical value reported in Fig. 1 of Hendrick and Edge (1966). To compare modeled neutron fluxes to observed neutron counts, the parameter N_s (Neutron saturation value, count h^{-1}), which represents the cosmic-ray neutron count rate normalized to that over water, must be specified.

2.4 Modeled neutron intensity for variations in pore water

To model variations in neutron intensity due to variable pore water profiles, we coupled a 1-D solution of the Richards equation to MCNPx. Full details of the experiment are reported in Franz et al. (2012a) who simulated one complete infiltration and drying cycle in four different soil textures: sand, sandy loam, silt, and silty clay loam. Fitting the same two-term exponential function found in Sect. 2.3 (Eq. 5) to the model results, the explained fraction of variance decreased from 99.5 to 96.5 % and the RMSE increased from 0.0639 to 0.0751 count count^{-1} (Fig. 2 and Table 1). The increased variation is due to the slight hysteresis that exists in the neutron intensity because of the vertical averaging of the sharp wetting front that exists during infiltration. The hysteresis is most pronounced in the coarser soils where sharp wetting fronts are strongest (Table 1).

2.5 Neutron intensity observations at Santa Rita Experimental Range

To further validate the universal calibration function, we compare observed neutron data with estimates of hydrogen molar fraction for five different volumetric calibration datasets (Table S1) and for continuous measurements from a distributed sensor network in Southern Arizona over a six-month period (details of the distributed sensor network observations are presented in Franz et al., 2012b). Continuous measurements were taken at depths of 10, 20, 30, 50, and 70 cm, in the same spatial pattern as the volumetric calibration samples. The same two-term exponential function as before (Eq. 5) yields N_s of 1019 count h^{-1} with an RMSE of 117.4 count h^{-1} and R^2 of 0.834 (Fig. 3, Table 1). The five volumetric sample data points are well fitted by the function, but there is a slight bias at the wet end for the distributed sensor network measurements. Because the shallowest soil moisture sensor was placed at 10 cm, the dynamics in the

HESSD
9, 10303–10322, 2012

top 5 cm are likely not well captured leading to a bias when shallow wetting fronts exist shortly after precipitation (Franz et al., 2012b). This problem does not exist with the moisture data from soil samples because the shallow layer soil moisture is captured adequately with the direct volumetric sampling method.

2.6 Neutron intensity observations at multiple sites

The analysis of forty-five calibration data sets from thirty-five different cosmic-ray neutron probe locations shows Eq. (5) accurately describes the data, with RMSE = 215 count h^{-1} and $R^2 = 0.756$ (Fig. 4b), over a wide range of soil moisture, soil bulk density, lattice water, vegetation, and water vapor conditions. As a direct comparison with Eq. (1), we find the best fit between total soil water $\left(\theta + \frac{\rho_{bd}}{\rho_w}\tau\right)$ and the observed neutrons counts had an RMSE = 286.4 count h^{-1} and $R^2 = 0.568$ (Fig. 4a). By including the differences in AGB between sites, Eq. (5) reduces RMSE from 286.4 to 215 count h^{-1} and increases R^2 from 0.568 to 0.756.

Looking at the residuals between Eq. (5) and observed values we find two sets of data that account for a large portion of the remaining uncertainty. The first subset comprises three sites where the observed hydrogen molar fraction is greater than the liquid water case at ~ 0.23. Above this value the count rate becomes flat, as the neutron probe is no longer sensitive to hydrogen being gained or lost to the system. The second subset of data is four sites where large forests grow in dry sandy soils supported by shallow water tables (Southeastern USA and Northern Michigan); it will be discussed in the next section.

3 Remaining uncertainties

Numerical and observational results show that the overall uncertainty using the cosmic-ray method to detect time varying hydrogen signals is small for a range of expected conditions (Table 1). The largest uncertainty resulted from the analysis of the forty-five

HESSD
9, 10303–10322, 2012

calibration data sets where we found that Eq. (5) does not fully capture sites that have large amounts of above ground biomass in dry soil moisture environments. In this work, the vegetation is presented as an equivalent layer of cellulose and water. However, as described in Sect. 2.1, the distribution of hydrogen above the surface may need to be explicitly accounted for in the life history of a neutron. Given the strong relationship for the five volumetric sample sets at Santa Rita Experimental Range (Fig. 3) (Franz et al., 2012b) and other local calibration functions (Desilets et al., 2010; Villarreyes et al., 2011), site-specific calibrations will implicitly include vegetation effects on observed neutron counts. But when comparing various sites with different geometries, there exists a small axis of variation that we are not properly accounting for with the equivalent layer assumption. Moreover, we do not include the effects of biomass below the ground surface, which may be significant but which is difficult to quantify. Future observational and theoretical work should aim to understand the effect on neutron intensity of biomass above and below ground surface. In terms of calibration datasets, accurate spatial estimates of volumetric water content may be difficult to obtain because of a large uncertainty in the determination of soil bulk density (Table S1) (Dane and Topp, 2002). Additional experimental work on accurate determinations of bulk density at intermediate spatial scales will help reduce the uncertainty in the cosmic-ray moisture measurements.

4 Outlook

With the presented framework, accurate estimates of soil moisture at difficult sampling sites or many points when using mobile surveys are now possible using cosmic-ray neutron probes. The proposed method requires ancillary data on location (for the computation of the incident cosmic-ray intensity), surface pressure, air temperature, and relative humidity to perform the necessary neutron intensity correction factors. In addition, estimates of soil bulk density and total biomass are needed, but spatially contiguous data are readily available from various sources. The most challenging aspect

HESSD
9, 10303–10322, 2012

is a spatial map of lattice water. Here we provide data from fifty sites (Table S2), but additional measurements along the mobile survey need to be made or, alternatively, relationships between bulk density and more readily available properties (Greacen, 1981) need to be established. Fig. 5 illustrates the expected neutron count rates solving Eqs. (3)–(5) for different combinations or pore water, lattice water, and above ground biomass, thus providing a local calibration function in order to estimate pore water.

In addition to computing pore water from the neutron intensity measurements, it is possible to isolate any of the other hydrogen signals (Fig. 5). This has potential applications to mapping total biomass or changes in biomass, which could be used as validation datasets for remote-sensing products (Lu et al., 2012; Weiss et al., 2007) or helping understand the carbon cycle dynamics. Furthermore, it may be possible to isolate the fraction of the total neutron signal that corresponds to an exchange of water from the surface to the atmosphere. It is the exchange of all water from the surface that will influence the transfer of mass, momentum, and energy, and this total exchangeable water is the critical climatic variable in interactions between land surface and the atmosphere and in ecosystem processes.

Supplementary material related to this article is available online at: http://www.hydrol-earth-syst-sci-discuss.net/9/10303/2012/ hessd-9-10303-2012-supplement.zip.

Acknowledgements. This research and the COSMOS project were supported by the US National Science Foundation under grant AGS-0838491. We would also like to thank, COSMOS site collaborators, Darin Desilets, Gary Womack, and Santa Rita Experimental Range for their support.

HESSD
9, 10303–10322, 2012

References

Dane, J. H. and Topp, C. G.: Methods of Soil Analysis: Part 4, Physical Methods, Soil Science Society of America, Madison, WI, USA, 2002.

Desilets, D., Zreda, M., and Ferre, T. P. A.: Nature's neutron probe: land surface hydrology at an elusive scale with cosmic rays, Water Resour. Res., 46, W11505, doi:10.1029/2009wr008726, 2010.

Franz, T. E., Zreda, M., Ferre, P. A., Rosolem, R., Zweck, C., Stillman, S., Zeng, X., and Shuttleworth, W. J.: Measurement depth of the cosmic-ray soil moisture probe affected by hydrogen from various sources, Water Resour. Res., 48, W08515, doi:10.1029/2012WR011871, 2012a.

Franz, T. E., Zreda, M., Rosolem, R., and Ferre, P. A.: Field validation of cosmic-ray soil moisture sensor using a distributed sensor network, Vadose Zone J., online first: https://www.soils.org/publications/vzj/first-look (last access: 7 September 2012), 2012b.

Greacen, E. L.: Soil Water Assessment by the Neutron Method, CSIRO, Melbourne, 1981.

Hendrick, L. D. and Edge, R. D.: Cosmic-ray neutrons near earth, Phys. Rev., 145, 1023–1025, doi:10.1103/PhysRev.145.1023, 1966.

Hornbuckle, B., Irvin, S., Franz, T. E., Rosolem, R., and Zweck, C.: The potential of the COSMOS network to be a source of new soil moisture information for SMOS and SMAP, paper presented at Proc. IEEE Intl. Geosci. Remote Sens. Symp., Munich, Germany, 2012.

Jung, M., Reichstein, M., Ciais, P., Seneviratne, S. I., Sheffield, J., Goulden, M. L., Bonan, G., Cescatti, A., Chen, J. Q., de Jeu, R., Dolman, A. J., Eugster, W., Gerten, D., Gianelle, D., Gobron, N., Heinke, J., Kimball, J., Law, B. E., Montagnani, L., Mu, Q. Z., Mueller, B., Oleson, K., Papale, D., Richardson, A. D., Roupsard, O., Running, S., Tomelleri, E., Viovy, N., Weber, U., Williams, C., Wood, E., Zaehle, S., and Zhang, K.: Recent decline in the global land evapotranspiration trend due to limited moisture supply, Nature, 467, 951–954, doi:10.1038/nature09396, 2010.

Knyazikhin, Y., Martonchik, J. V., Myneni, R. B., Diner, D. J., and Running, S. W.: Synergistic algorithm for estimating vegetation canopy leaf area index and fraction of absorbed photosynthetically active radiation from MODIS and MISR data, J. Geophys. Res.-Atmos., 103, 32257–32275, doi:10.1029/98jd02462, 1998.

HESSD
9, 10303–10322, 2012

Koster, R. D., Dirmeyer, P. A., Guo, Z. C., Bonan, G., Chan, E., Cox, P., Gordon, C. T., Kanae, S., Kowalczyk, E., Lawrence, D., Liu, P., Lu, C. H., Malyshev, S., McAvaney, B., Mitchell, K., Mocko, D., Oki, T., Oleson, K., Pitman, A., Sud, Y. C., Taylor, C. M., Verseghy, D., Vasic, R., Xue, Y. K., Yamada, T., and Team, G.: Regions of strong coupling between soil moisture and precipitation, Science, 305, 1138–1140, doi:10.1126/science.1100217, 2004.

Lu, D., Chen, Q., Wang, G., Moran, E., Batistella, M., Zhang, M., Laurin, G. V., and Saah, D.: Aboveground forest biomass estimation with Landsat and LiDAR data and uncertainty analysis of the estimates, Int. J. Forest. Res., 2012, 436537, doi:10.1155/2012/436537, 2012.

Pelowitz, D. B. (Ed.): MCNPX User's Manual, version 5, Rep. LA-CP-05-0369, Los Alamos National Laboratory, Los Alamos, 2005.

Robinson, D. A., Binley, A., Crook, N., Day-Lewis, F. D., Ferre, T. P. A., Grauch, V. J. S., Knight, R., Knoll, M., Lakshmi, V., Miller, R., Nyquist, J., Pellerin, L., Singha, K., and Slater, L.: Advancing process-based watershed hydrological research using near-surface geophysics: a vision for, and review of, electrical and magnetic geophysical methods, Hydrol. Process., 22, 3604–3635, 2008.

Rosolem, R., Shuttleworth, W. J., Zreda, M., Franz, T. E., and Zeng, X.: The effect of atmospheric water vapor on the cosmic-ray soil moisture signal, J. Hydrometeorol., in review, 2012.

Seneviratne, S. I., Corti, T., Davin, E. L., Hirschi, M., Jaeger, E. B., Lehner, I., Orlowsky, B., and Teuling, A. J.: Investigating soil moisture-climate interactions in a changing climate: a review, Earth Sci. Rev., 99, 125–161, doi:10.1016/j.earscirev.2010.02.004, 2010.

Topp, G. C., Davis, J. L., and Annan, A. P.: Electromagnetic determination of soil-water content – measurements in coaxial transmission-lines, Water Resour. Res., 16, 574–582, 1980.

Rivera Villarreyes, C. A., Baroni, G., and Oswald, S. E.: Integral quantification of seasonal soil moisture changes in farmland by cosmic-ray neutrons, Hydrol. Earth Syst. Sci., 15, 3843–3859, doi:10.5194/hess-15-3843-2011, 2011.

Wang, A. H., Zeng, X. B., Shen, S. S. P., Zeng, Q. C., and Dickinson, R. E.: Time scales of land surface hydrology, J. Hydrometeorol., 7, 868–879, doi:10.1175/jhm527.1, 2006.

Weiss, M., Baret, F., Garrigues, S., and Lacaze, R.: LAI and fAPAR CYCLOPES global products derived from VEGETATION, Part 2: Validation and comparison with MODIS collection 4 products, Remote Sens. Environ., 110, 317–331, doi:10.1016/j.rse.2007.03.001, 2007.

Zreda, M., Desilets, D., Ferre, T. P. A., and Scott, R. L.: Measuring soil moisture content non-invasively at intermediate spatial scale using cosmic-ray neutrons, Geophys. Res. Lett., 35, L21402, doi:10.1029/2008gl035655, 2008.
Zreda, M., Shuttleworth, W. J., Zeng, X., Zweck, C., Desilets, D., Franz, T., Rosolem, R., and Ferre, T. P. A.: COSMOS: The COsmic-ray Soil Moisture Observing System, Hydrol. Earth Syst. Sci. Discuss., 9, 4505–4551, doi:10.5194/hessd-9-4505-2012, 2012.

HESSD
9, 10303–10322, 2012

Table 1. Summary of coefficients and fitting statistics for modeled and observed cases.

Case	RMSE (count h^{-1})	R^2	a^a	b^a	c^a	d^a	N_s^a
Poisson Counting Uncertainty for 6 h average period (1000 to 2500 count h^{-1})	12.9 to 20.4	NA	NA	NA	NA	NA	NA
Modeled Variable Chemistry	63.9[b]	0.995	4.264	−49.4	4.382	−6.401	NA
Modeled Variable Pore Water Profiles, all	75.1[b]	0.965	4.114	−49.4	4.228	−6.401	NA
Modeled Variable Pore Water Profiles, sand	107.0[b]	0.855	4.091	−49.4	4.204	−6.401	NA
Modeled Variable Pore Water Profiles, sandy loam	78.4[b]	0.831	4.184	−49.4	4.300	−6.401	NA
Modeled Variable Pore Water Profiles, silt	39.3[b]	0.783	4.107	−49.4	4.221	−6.401	NA
Modeled Variable Pore Water Profiles, silty clay loam	39.8[b]	0.447	4.058	−49.4	4.171	−6.401	NA
Modeled Chemistry and Pore Water Profiles[c]	83.8[b]	0.989	4.486	−48.1	4.195	−6.181	NA
Observed, Santa Rita Experimental Range	117.4	0.834	4.486	−48.1	4.195	−6.181	1019.0
Observed, Forty-Five Calibration Datasets	215	0.756	4.486	−48.1	4.195	−6.181	992.6

[a] Coefficients for Eq. (5), $N/N_s = a \times \exp(b \times \text{hmf}) + c \times \exp(d \times \text{hmf})$.
[b] Assuming N_s = 1000 count h^{-1}.
[c] Coefficients used in all figures and observed fitting.

Discussion Paper | Discussion Paper | Discussion Paper | Discussion Paper |

HESSD
9, 10303–10322, 2012

Calibration function for soil moisture determination with cosmic-ray neutrons

T. E. Franz et al.

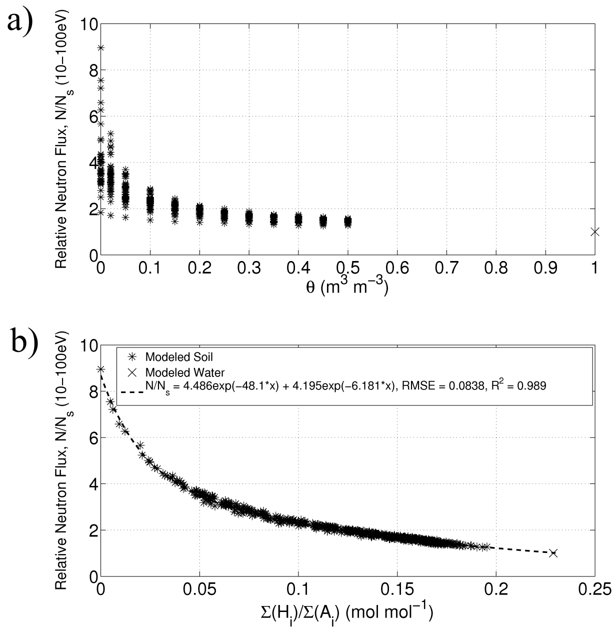

Fig. 1. MCNPx modeled relative neutron flux versus **(a)** twelve uniformly distributed pore water content profiles (0, 0.02, 0.05, 0.10, 0.15, 0.20, 0.25, 0.30, 0.35, 0.40, 0.45, 0.50 $m^3 m^{-3}$) and **(b)** computed hydrogen molar fraction in the support volume of cosmic-ray neutron probe for fifty different observed soil mineral chemistries at COSMOS sites (Table S2). The horizontal axis in **(b)** is the ratio of the sum of all hydrogen moles that are present in the support volume (vegetation, pore water, and soil mineral water) and the sum of all moles from all elements that are present in air, vegetation, soil, and pore water. Note the combined modeled chemistry and pore water profile cases were used for the best curve fitting analysis (see Table 1 for individual data fits).

HESSD
9, 10303–10322, 2012

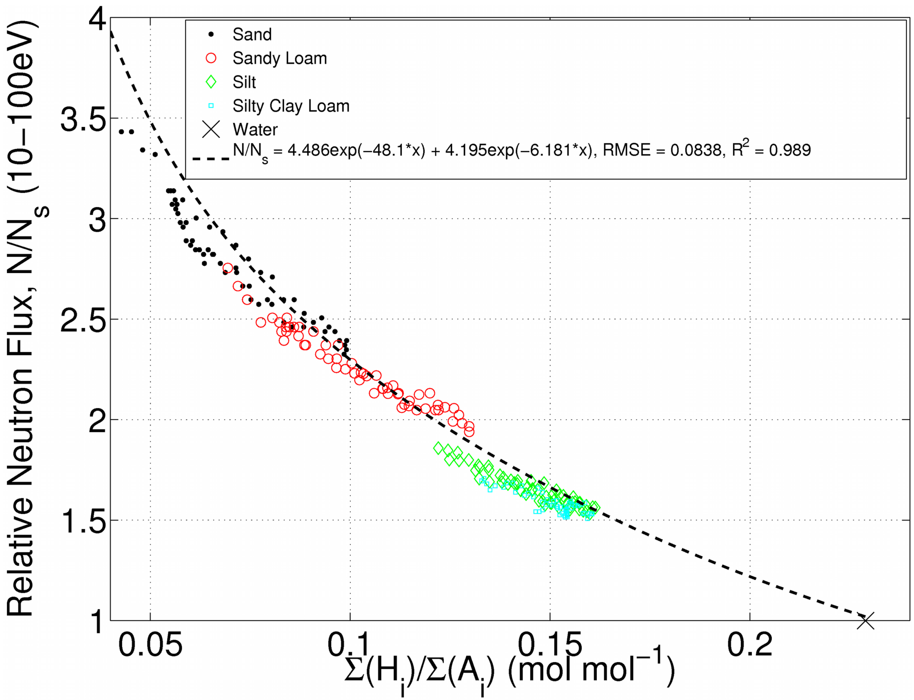

Fig. 2. MCNPx modeled neutron flux versus hydrogen molar fraction for four different soil textures undergoing one wetting and drying cycle. Each soil moisture profile was generated using a numerical solution to the 1-D Richards equation for a top boundary condition of a 2.54 cm rain event that lasted 24 h followed by a 2 mm d^{-1} potential evapotranspiration for 9 days, a free drainage lower boundary condition, initial condition set to field capacity, and a vertical resolution of 2 cm. Note the combined modeled chemistry and pore water profile cases were used for the best curve fitting analysis (see Table 1 for individual data fits).

HESSD
9, 10303–10322, 2012

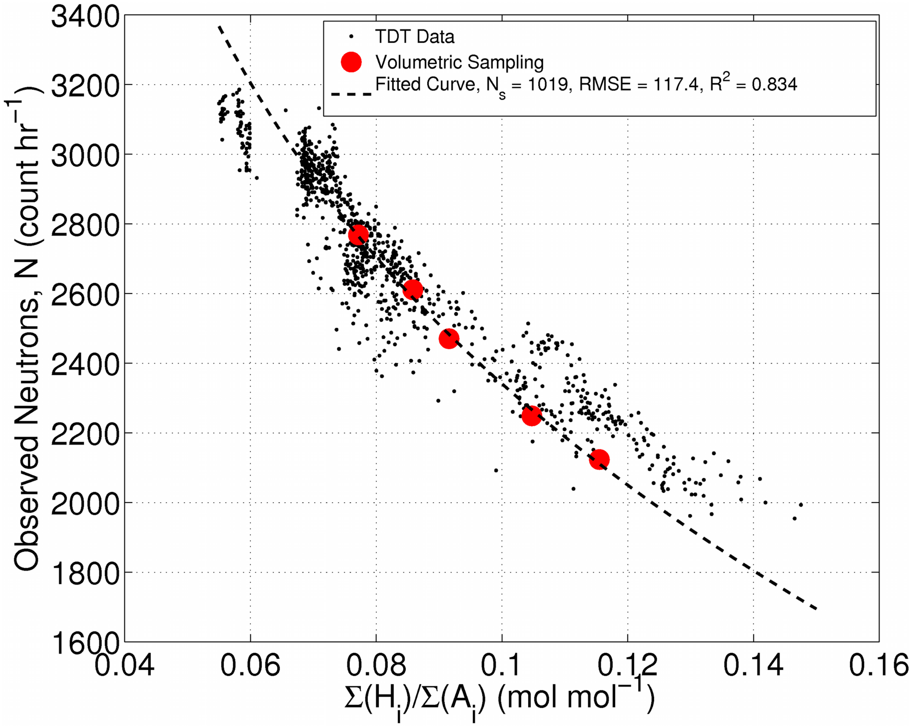

Fig. 3. Observed neutron counts and computed hydrogen molar fractions from five sets of multiple soil samples collected for calibration purposes at five different times, and continuous measurements from a network of time-domain transmission sensors (TDT, Acclima Inc. Meridian, ID, USA) from 1 July 2011 to 5 January 2012, at Santa Rita Experimental Range in Southern Arizona (31.9085° N 110.8394° W). See Table S1 for calibration datasets.

HESSD

9, 10303–10322, 2012

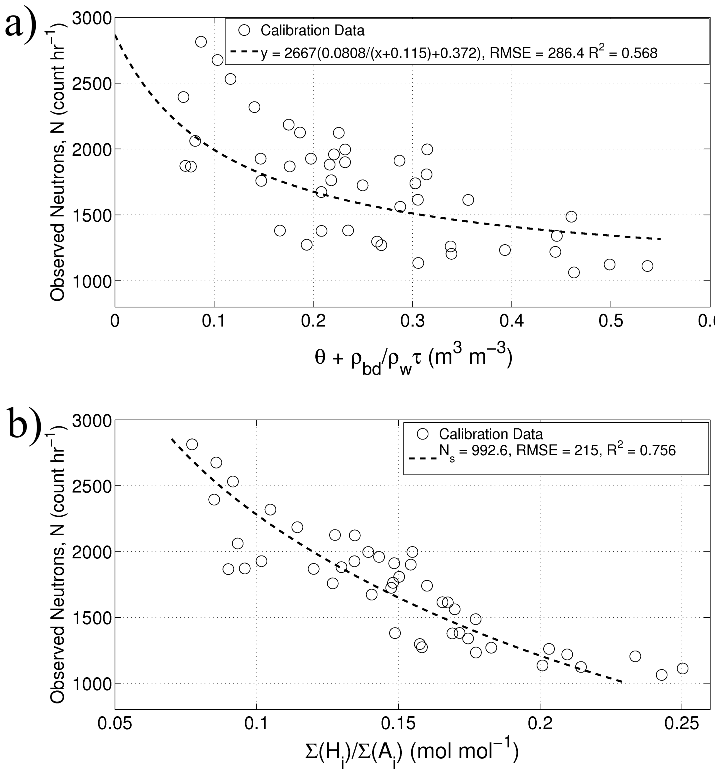

Fig. 4. Observed neutron counts versus **(a)** total soil water and **(b)** hydrogen molar fraction from forty-five calibration datasets at thirty-five different cosmic-ray neutron probes. See Table S1 for calibration datasets.

HESSD
9, 10303–10322, 2012

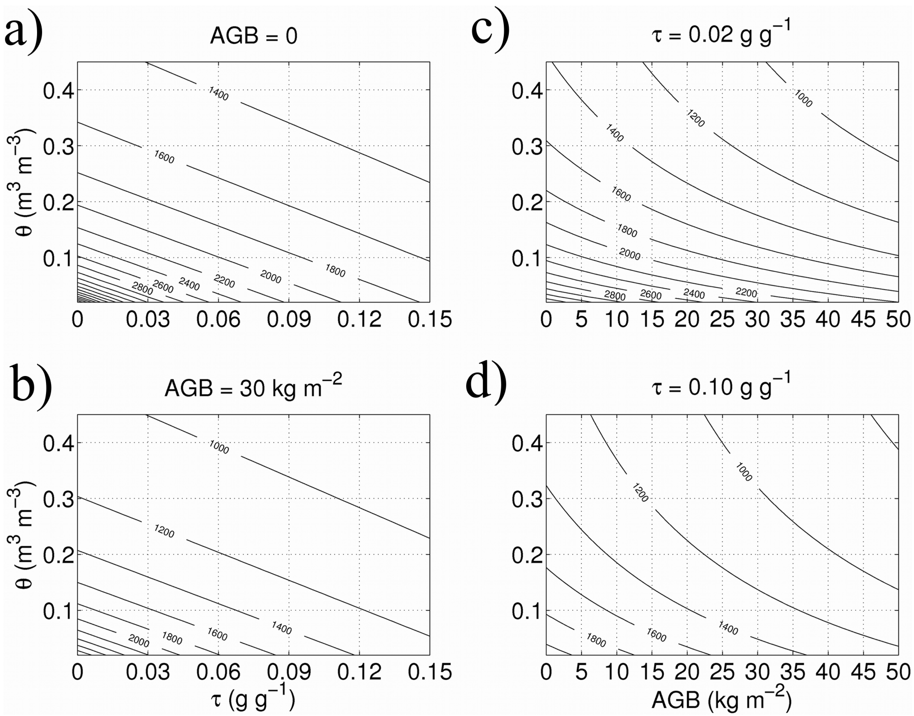

Fig. 5. Contours of predicted neutron counts (count h^{-1}) using Eqs. (3)–(5), bulk density = 1.4 g cm^{-3}, and N_s = 1000 count h^{-1} for **(a)** and **(b)** a range of pore and lattice water values and two different above ground biomass cases and for **(c)** and **(d)** a range pore water and above ground biomass values for two different lattice water cases.

HESSD
9, 10303–10322, 2012

T. E. Franz et al.